Full-frequency voltage noise spectral density of a single-electron transistor

Andreas Käck and Göran Wendin
Microtechnology Center at Chalmers MC2, Department of Microelectronics and Nanoscience, Chalmers University of Technology and Göteborg University, S-412 96, Göteborg, Sweden

Göran Johansson
Institut für Theoretische Festkörperphysik, Universität Karlsruhe, D-761 28 Karlsruhe, Germany
(Received 6 October 2002; published 6 January 2003)

We calculate the full-frequency spectral density of voltage fluctuations in a single-electron transistor (SET), used as an electrometer biased above the Coulomb threshold so that the current through the SET is carried by sequential tunneling events. We consider both a normal-state SET and a superconducting SET. The whole spectrum, from low-frequency telegraph noise to quantum noise at frequencies comparable to the SET charging energy ($E_C/\hbar$) to high-frequency Nyquist noise, is described. We take the energy exchange between the SET and the measured system into account using a real-time diagrammatic Keldysh technique. The voltage fluctuations determine the backaction of the SET on the measured system, and we specifically discuss the case of superconducting charge qubit read-out and measuring the so-called Coulomb staircase of a single Cooper-pair box.

DOI: 10.1103/PhysRevB.67.035301 PACS number(s): 73.23.Hk, 03.67.Lx, 42.50.Lc, 85.25.Na

I. INTRODUCTION

Solid-state realizations of qubits are of real interest due to the possibility of using lithographic techniques to integrate the large number of qubits, needed for a fully functional QC. The single-electron transistor (SET) has been suggested as a read-out device for different solid-state charge qubits.[1–5]

Aassime *et al.*[1] have shown that the radio-frequency SET (Ref. 6) (rf SET) may be used for single shot read-out of the single cooper-pair Box (SCB) qubit.[7,8] This is possible if the measurement time $t_{\rm ms}$ needed to resolve the two states of the qubit is much shorter than the time $t_{\rm mix}$ on which the qubit approaches its new steady-state determined by the back-action due to voltage fluctuations on the SET. In a previous short paper[9] we provided further support for this result by calculating the full frequency voltage noise spectral density of the SET, including the effect of energy exchange between the qubit and the SET.

In this paper we give a full account of the calculation as well as a thorough discussion of the effect of back action in measuring the so-called Coulomb staircase of an SCB qubit. We also include a section about the back action from a superconducting SET.

Since the qubit is carefully shielded from all unwanted interactions with its environment it is reasonable to assume that the back action from the SET charge measurement is the dominating noise source, even though the two systems are only weakly coupled. This further motivates choosing measurements on a charge qubit to discuss the spectral properties of SET back action, compare, e.g., Ref. 10. In nonqubit systems, e.g., a normal-state single-electron box, other sources of dissipation dominate over the back action from the charge measurement. Furthermore we do not discuss the dephasing of the qubit induced by the presence of the SET.[11,12] Although it is a very important subject, the dephasing time is mainly determined by the zero frequency fluctuations, and in this limit our result coincides with previous expressions.[13]

The structure of the paper is the following. In Sec. II we discuss the basic properties of the SCB qubit and the effect of gate voltage fluctuations. Furthermore the difference between asymmetric and symmetric definitions of noise spectral density is noted and also the connection to mixing time and the Coulomb staircase. In Sec. III the model for the SET is introduced and in Sec. IV the real-time diagrammatic Keldysh technique is described and the expression for the spectral density of voltage fluctuations on the SET island is derived. Section V describes the properties of the voltage fluctuations in different frequency regimes, the effect on the mixing time and the Coulomb staircase both for a normal-state SET and a superconducting SET.

II. THE SINGLE COOPER-PAIR BOX QUBIT

The qubit is here made up of the two lowest lying energy levels in a single Cooper-pair box (SCB) (see Fig. 1).[7] An SCB is a small superconducting island coupled to a superconducting reservoir via a Josephson junction. The Hamiltonian of the system can be written in the charge basis as[12]

$$H_q=\sum_n 4E_{\rm qb}(n-n_g)^2|n\rangle\langle n| - \frac{E_J}{2}[|n\rangle\langle n+1|+|n+1\rangle\langle n|], \quad (1)$$

where $E_{\rm qb}=e^2/C_{\rm qb}$ is the charging energy, n is the number of extra Cooper pairs on the island, E_J is the Josephson energy of the junction and $n_g=C_g^{\rm qb}V_g^{\rm qb}/2e$ is the number of gate-induced Cooper pairs. In order to get a good Cooper-pair box we need $k_BT\ll E_J\ll E_c<\Delta$, where Δ is the superconducting gap and T is the temperature. The low temperature is required to prevent thermal excitations and the high superconducting gap is needed to suppress quasiparticle tunneling. The eigenenergies now form parabolas, varying with the gate

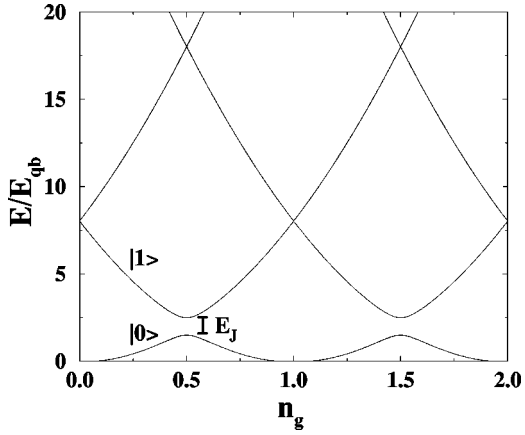

FIG. 1. The energy bands of an SCB. The states $|0\rangle$ and $|1\rangle$ denote the eigenstates on the island. The quasiparticle branches have been left out for simplicity. The gap is due to hybridization of the charge states by the Josephson coupling.

voltage. For suitable values of the gate voltage (close to $n_g = 1/2$), and for $E_J \ll E_c$, the system reduces to an effective two level system as the two lowest lying charge states are well separated from the states with higher energy. Including only the two lowest lying states in Eq. (1) the qubit Hamiltonian becomes

$$H_q = -\frac{4E_{\rm qb}}{2}(1-2n_g)\sigma_z - \frac{E_J}{2}\sigma_x, \tag{2}$$

where $\sigma_{x,z}$ are the Pauli matrices (and the states $|\uparrow\rangle = \binom{1}{0}$ and $|\downarrow\rangle = \binom{0}{1}$ correspond to zero and one extra Cooper pair on the qubit island). By changing the gate voltage the eigenstates of the qubit can be tuned from being almost pure charge states to a superposition of charge states.

The ground state/first excited state of the system, written in the charge basis ($E_J = 0$) are

$$|0\rangle = \cos(\eta/2)|\uparrow\rangle + \sin(\eta/2)|\downarrow\rangle,$$

$$|1\rangle = -\sin(\eta/2)|\uparrow\rangle + \cos(\eta/2)|\downarrow\rangle, \tag{3}$$

where $\eta = \arctan[E_J/4E_{\rm qb}(1-2n_g)]$ is the mixing angle. The energy difference between the two states is $\Delta E = \sqrt{(4E_{\rm qb})^2(1-2n_g)^2 + E_J^2}$ and the average charge of the eigenstates is

$$Q_0 = 2e|\langle\downarrow|0\rangle|^2 = 2e\sin^2(\eta/2),$$

$$Q_1 = 2e|\langle\downarrow|1\rangle|^2 = 2e\cos^2(\eta/2). \tag{4}$$

A. Qubit transitions induced by SET voltage fluctuations

When the SET is turned on in order to measure the qubit, the voltage fluctuations on the SET island induce a fluctuating charge on the qubit island. This is equivalent to a fluctuating qubit gate charge $n_g \to n_g + \delta n_g(t)$, giving rise to a fluctuating term in the qubit Hamiltonian, written in the charge basis as

$$\delta H_q(t) = \frac{4E_{\rm qb}}{2} 2\,\delta n_g(t)\sigma_z = 2e\kappa\,\delta V(t)\sigma_z, \tag{5}$$

where $\kappa = C_c/C_{\rm qb}$. Here $\delta V(t)$ represents the voltage fluctuations on the SET island, and we have neglected a term quadratic in $\delta n_g(t)$. In the qubit eigenbasis, using the rotation defined by Eq. (3), the fluctuations in Eq. (5) become

$$\delta H(t) = 2e\kappa\,\delta V(t)[\cos(\eta)\sigma_z + \sin(\eta)\sigma_x]. \tag{6}$$

The fluctuating voltage on the SET island can induce transitions between the eigenstates of the qubit. If the capacitive coupling to the SET is small ($\kappa \ll 1$) we can use the Fermi golden rule to calculate the transition rates

$$\Gamma_{\rm rel}(\Delta E) = \frac{e^2}{\hbar^2}\frac{E_J^2}{\Delta E^2}\kappa^2 S_V(\Delta E/\hbar), \tag{7}$$

$$\Gamma_{\rm exc}(\Delta E) = \frac{e^2}{\hbar^2}\frac{E_J^2}{\Delta E^2}\kappa^2 S_V(-\Delta E/\hbar), \tag{8}$$

where $\Gamma_{\rm rel}$ is the relaxation rate and $\Gamma_{\rm exc}$ is excitation rate and $S_V(\Delta E)$ is the asymmetric [see Eq. (9)] spectral density of the voltage fluctuations on the SET island. The fraction $E_J/\Delta E = \sin(\eta)$ comes from Eq. (6) as it is only σ_x that causes any transitions between the states. Note that the $\cos(\eta)\sigma_z$ term causes fluctuation of the energy levels, leading to phase fluctuations and dephasing.

B. Asymmetric noise—Coulomb staircase

In our calculations we emphasize the energy exchange between the qubit and the SET and separate between the contributions from processes leading to the qubit loosing energy and the contribution from processes leading to the qubit gaining energy (or, equivalently, the SET absorbing or emitting energy). Because of this, we will maintain this separation of the noise spectral density of the SET into contributions from positive and negative frequencies and therefore use the asymmetric expression for the voltage fluctuations

$$S_V(\omega) = \int_{-\infty}^{\infty} e^{-i\omega\tau}\langle\delta V(\tau)\,\delta V(0)\rangle. \tag{9}$$

As we are primarily interested in the processes in the SET we chose our reference so that positive frequencies correspond to the SET absorbing energy and negative frequencies correspond to the SET emitting energy.

One example where the separation is necessary is in describing the back action of the SET while measuring the so-called Coulomb staircase, i.e., the average charge of the qubit as a function of its gate voltage. In an ideal situation with no energy available from an external source, at zero temperature, the qubit would follow the ground state adiabatically and the charge would increment in steps of $2e$ at $n_g = n + 0.5$, n integer. These steps are not perfectly sharp because of the Josephson energy mixing the charge states. This mixing of charge states results in a maximal derivative given by $4E_C/E_J$.[7] When adding a noise source, e.g., by

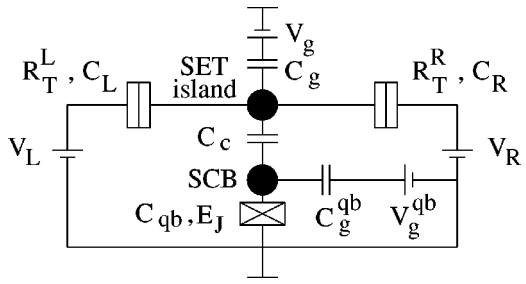

FIG. 2. The SET.

increasing the temperature or attaching a noisy measurement device, the steps will be rounded further due to a finite population of the excited state.

Assuming that the SET is the dominant noise source, and that the two state approximation of the qubit is valid, the steady-state population of the qubit is given by

$$P_1^{\mathrm{st,qb}}=\Gamma_{\mathrm{exc}}(\Delta E)/[\Gamma_{\mathrm{exc}}(\Delta E)+\Gamma_{\mathrm{rel}}(\Delta E)] \tag{10}$$

$$P_0^{\mathrm{st,qb}}=\Gamma_{\mathrm{rel}}(\Delta E)/[\Gamma_{\mathrm{exc}}(\Delta E)+\Gamma_{\mathrm{rel}}(\Delta E)]. \tag{11}$$

The corresponding expression for the average charge is then given by

$$Q(\Delta E)=Q_0(\Delta E)P_0^{\mathrm{st,qb}}(\Delta E)+Q_1(\Delta E)P_1^{\mathrm{st,qb}}(\Delta E), \tag{12}$$

where $Q_{\uparrow/\downarrow}$ is the charge of the excited state/ground state defined in Eq. (4). If we set $P_1^{\mathrm{st,qb}}=0$ and $P_0^{\mathrm{st,qb}}=1$, we recover the ideal Coulomb staircase, as this corresponds to the system following the ground state adiabatically.

C. Symmetric noise—Mixing time

For quantities that depend on the summed rate of relaxation and excitation processes in the SET the separation of absorption and emission might not be necessary, and the symmetrised expression for voltage fluctuations

$$S_V^{\mathrm{sym}}(\omega)=\int_{-\infty}^{\infty}d\tau e^{-i\omega\tau}\langle\delta V(\tau)\delta V(0)+\delta V(0)\delta V(\tau)\rangle \tag{13}$$

can be used. Note that $S_V^{\mathrm{sym}}(\omega)=S_V(\omega)+S_V(-\omega)$.

One example is the time it takes the qubit to reach its steady state, after the SET is switched on. This time is called the mixing time, and the information about the initial state population is lost on this timescale. For weak coupling it is[11,12]

$$\frac{1}{\tau_{\mathrm{mix}}}=\Gamma_{\mathrm{rel}}(\Delta E)+\Gamma_{\mathrm{exc}}(\Delta E)\propto S_V^{\mathrm{sym}}(\Delta E/\hbar). \tag{14}$$

III. SET MODEL

We follow the outline of Ref. 14 and model the SET (see Fig. 2) by the Hamiltonian

$$H=H_L+H_R+H_I+V+H_T=H_0+H_T, \tag{15}$$

where

$$H_r=\sum_{kn}\epsilon_{kn}^r a_{krn}^\dagger a_{krn}, \quad H_I=\sum_{ln}\epsilon_{ln}c_{ln}^\dagger c_{ln} \tag{16}$$

describe noninteracting electrons in the left/right lead ($H_r, r\in\{L,R\}$) and on the island (H_I). The quantum numbers n denote transverse channels including spin, and k,l denote momenta. The Coulomb interaction on the island is described by

$$V(\hat{N})=E_C(\hat{N}-n_x)^2, \tag{17}$$

where $\hat{N}$ denotes the excess number operator, $E_C=e^2/2C$ the charging energy ($C=C_L+C_R+C_g+C_c$), n_x the fractional number of electrons induced by the external voltages [n_x is the fractional part of $(C_LV_L+C_RV_R+C_gV_g)/e$], and e the electron charge. The tunneling term is

$$\begin{aligned}H_T&=\sum_{r=L,R}\sum_{kln}(T_{kl}^{rn}a_{krn}^\dagger c_{ln}e^{-i\hat{\Phi}}+T_{kl}^{rn*}c_{ln}^\dagger a_{krn}e^{i\hat{\Phi}})\\&=H^-+H^+,\end{aligned} \tag{18}$$

where the operator $e^{\pm i\hat{\Phi}}$ changes the excess particle number on the island by ±1 and T_{kl}^{rn} are the tunneling matrix elements. $\hat{\Phi}$ is the canonical conjugate to $\hat{N}$,$([\hat{\Phi},\hat{N}]=i)$. In this case of a metallic island containing a large number of electrons, the charge degree of freedom $N=0,\pm1,\ldots,$ is to a very good approximation independent of the electron degrees of freedom l,n. The terms H^+ and H^- represent electron tunneling to and from the SET island. The form of the tunneling terms (with the $e^{i\hat{\Phi}}$ term) is a consequence of separating state space into electron l, n, and charge N degrees of freedom. This is also reflected in the partitioning of the density matrix introduced below.

The spectral density of voltage fluctuations on the SET island is described by the Fourier transform of the voltage-voltage correlation function

$$\begin{aligned}S_V(\omega)&=\frac{e^2}{C^2}\int_{-\infty}^{\infty}d\tau e^{-i\omega\tau}\,\mathrm{Tr}\{\rho_{\mathrm{st}}(t_0)\delta\hat{N}(\tau)\delta\hat{N}(0)\}\\&=\frac{e^2}{C^2}\int_{-\infty}^{\infty}d\tau e^{-i\omega\tau}\,\mathrm{Tr}\{\rho_{\mathrm{st}}(t_0)[\hat{N}(\tau)\hat{N}(0)-\overline{N}^2]\},\end{aligned} \tag{19}$$

where $\overline{N}$ is the average of $\hat{N}$. The $\overline{N}^2$ term in Eq. (19) assures that the correlation function vanishes for large τ. In Fourier space this term does not contribute at finite frequency, and at zero frequency it compensates for the steady state delta function. In order to simplify our expressions we leave this term out, and keep the frequency finite during the calculations.

In Eq. (19) $\rho_{\mathrm{st}}(t_0)$ is the density matrix of the system in the steady-state, which is assumed to have been reached at some time t_0 before the fluctuation occurs ($t_0<\min\{0,\tau\}$).

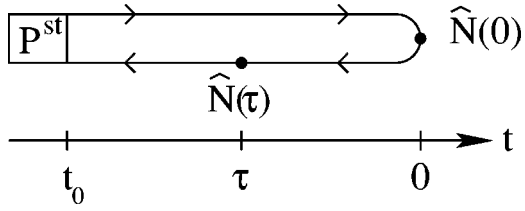

FIG. 3. The propagation of the unperturbed steady state density matrix. This corresponds to the first term in Eq. (22).

$\rho_{\rm st}=\rho^e_{\rm eq}\otimes\rho^c_{\rm st}$ is the tensor product of the equilibrium (Fermi distributed) density matrix $\rho^e_{\rm eq}$ for the electron degrees of freedom in each reservoir (L,R,I) and a reduced density matrix $\rho^c_{\rm st}$, describing the charge degrees of freedom. Since the tunneling events between the SET island and the electrodes are incoherent due to the low conductance of the tunnel junctions, the charge states will be incoherent, and $\rho^c_{\rm st}$ is therefore taken to be diagonal[15] with elements $P^{\rm st}_N$ denoting the steady-state probability of being in charge state N.

IV. DIAGRAMMATIC TREATMENT

We now expand the correlation function in Eq. (19) in a perturbation series in terms of the tunneling Hamiltonian (H_T) along a Keldysh time contour (see Fig. 3). The trace over the electron degrees of freedom is then evaluated using Wick's theorem, which is possible since the tunneling Hamiltonian is only bilinear in the fermionic operators. Rewriting Eq. (19) in the interaction picture gives (excluding the $\overline{N}^2$ term)

$$S_V(\omega)=\frac{e^2}{C^2}\int_{-\infty}^{\infty}d\tau e^{-i\omega\tau}\times{\rm Tr}\{\rho(t_0)S(t_0,\tau)\hat{N}(\tau)S(\tau,0)\hat{N}(0)S(0,t_0)\},\tag{20}$$

where $S(t_2,t_1)$ is the S matrix that brings the system from the time t_1 to time t_2, i.e., for $t_2>t_1$

$$S(t_2,t_1)=e^{-iT\int_{t_1}^{t_2}dtH_T(t)}=1-i\int_{t_1}^{t_2}d\tau_1H_T(\tau_1)+(-i)^2\int_{t_1}^{t_2}d\tau_1\int_{t_1}^{\tau_1}d\tau_1d\tau_2H_T(\tau_1)H_T(\tau_2)+\cdots,\tag{21}$$

and analogously for $t_2<t_1$. Defining T as the time-ordering operator along the Keldysh contour we can write Eq. (20) as

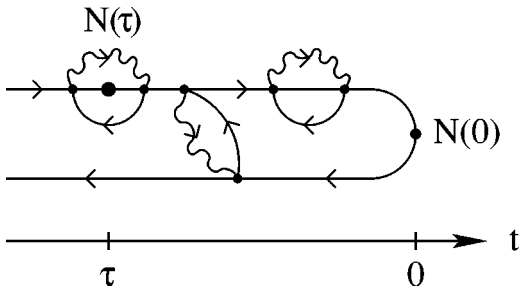

FIG. 4. An example of a specific diagram. The wiggly lines correspond to island lines and the solid lines correspond to lead lines. The right-most part correspond to an electron-hole excitation while the left-most part corresponds to a correction to the external vertex. The middle part corresponds to a tunneling event as only the diagrams connecting the upper and lower branch changes the number of extra charges on the island.

$$S_V(\omega)=\frac{e^2}{C^2}\int_{-\infty}^{\infty}d\tau e^{-i\omega\tau}\Big[{\rm Tr}\{\rho(t_0)\hat{N}(\tau)\hat{N}(0)\}-i\int_{-\infty}^{0}d\tau_1\,{\rm Tr}\{T\rho(t_0)\hat{N}(\tau)\hat{N}(0)H_T(\tau_1)\}+\frac{(-i)^2}{2!}\int_{-\infty}^{0}d\tau_1\int_{-\infty}^{0}d\tau_2\times{\rm Tr}\{T\rho(t_0)\hat{N}(\tau)\hat{N}(0)H_T(\tau_1)H_T(\tau_2)\}+\cdots\Big].\tag{22}$$

Since the unperturbed Hamiltonian does not contain any couplings between the leads and the island nor between the leads themselves, their degrees of freedom are independent. Moreover, as the trace of independent degrees of freedom is equal to the product of the respective traces and every perturbation term contains one operator from one of the leads and one operator from the island, only terms containing an even number of perturbation terms will contribute. Using the diagrammatic language of Ref. 14, the noise correlation function $S_V(\omega)$ can be given a diagrammatic formulation.

Figure 3 shows a diagrammatic representation of the first term in Eq. (22) with zero H_T perturbations, involving the evolution of the state described by the density matrix itself along the Keldysh time contour. This process is represented by a solid line starting and ending at the the density matrix, including the charge (fluctuation) operators $\hat{N}(\tau)$ and $\hat{N}(0)$ marked by dots. This gives the expectation value (statistical average) of the charge fluctuation correlation (in the ''ground state'') in the absence of any transport process.

The first contributions to charge transport come from the third term in Eq. (22) with one H^+ and one H^- perturbation, describing tunneling onto the SET island and back, changing the charge state N to $N\pm1$. A diagrammatic representation of this would be the middle part of Fig. 4. Since the charge-transfer process can be viewed as an electron-hole excitation, creating a hole on an electrode and an electron on the island,

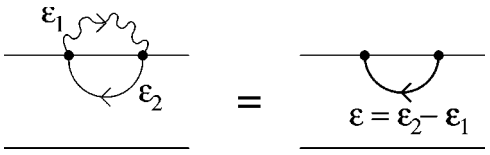

FIG. 5. Two internal electron lines with reversed start and end points. They can be replaced by a single line with an energy equal to the difference in energy between the two corresponding to an electron-hole excitation.

in Fig. 4 there are new additional lines with arrows representing electron-hole propagators (excitations). Every internal time will form a vertex and the propagator $\langle Ta(\tau_1)a^\dagger(\tau_2)\rangle$ will form a line going from τ_2 to τ_1. In this case with macroscopic metallic reservoirs with many transverse channels, the main contributing terms[14] will appear in combinations of

$$\langle TH^+(\tau_1)H^-(\tau_2)\rangle = \sum_{r_1}\sum_{r_2}\sum_{k_1 l_1 n_1}\sum_{k_2 l_2 n_2}[T^{r_1 n_1 *}_{k_1 l_1} T^{r_2 n_2}_{k_2 l_2} \times\langle Ta_{k_1 r_1 n_1}(\tau_1)a^\dagger_{k_2 r_2 n_2}(\tau_2)\rangle \times\langle Tc^\dagger_{k_1 r_1 n_1}(\tau_1)c_{k_2 r_2 n_2}(\tau_2)\rangle], \quad (23)$$

which means that there will always be pairs of internal lines with reversed start and end points, one being a reservoir propagator and one being an island propagator, as shown in Fig. 5. These line-pairs are replaced by a single line, corresponding to an electron-hole excitation, with an energy equal to the difference in energy between the two lines.

In order to facilitate the evaluation of the time-ordered diagrams in Eq. (22), we rewrite the Fourier transform in Eq. (19) as

$$\begin{aligned} S_V(\omega) &= \frac{e^2}{C^2}\int_{-\infty}^{\infty} d\tau e^{-i\omega\tau}\mathrm{Tr}\{\rho_{\mathrm{st}}(t_0)\hat{N}(\tau)\hat{N}(0)\} \\ &= \frac{e^2}{C^2}\int_{-\infty}^{0} d\tau e^{-i\omega\tau}\mathrm{Tr}\{\rho_{\mathrm{st}}(t_0)\hat{N}(\tau)\hat{N}(0)\} \\ &\quad + \frac{e^2}{C^2}\int_{-\infty}^{0} d\tau e^{+i\omega\tau}\mathrm{Tr}\{\rho_{\mathrm{st}}(t_0)\hat{N}(0)\hat{N}(\tau)\} \\ &= 2\frac{e^2}{C^2}\mathrm{Re}\left[\int_{-\infty}^{0} d\tau e^{-i\omega\tau}\mathrm{Tr}\{\rho_{\mathrm{st}}(t_0)\hat{N}(\tau)\hat{N}(0)\}\right], \end{aligned} \quad (24)$$

where we have used that the steady-state is time invariant. Furthermore we fix the specific time ordering of all internal and external times in all diagrams. This make the diagrams straightforward to evaluate in the frequency domain as all integrals thus become recursive Laplace transforms. Returning to Eq. (22) and drawing all the diagrams of the lowest nontrivial order we can divide them into two categories: Dressings of the propagator $\Pi_{N,N'}(\omega)$ that takes the system from the charge state N to the state N' (see Fig. 6) and vertex correction (see Fig. 7).

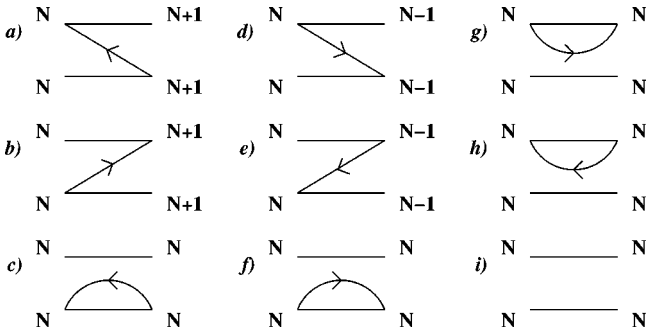

FIG. 6. All the diagrams that enter the propagator, to the lowest order.

Calculating for instance, the diagram in Fig. 6(h) using the diagrammatic technique outlined in Ref. 14 yields

$$D_N = -\sum_r \lim_{\eta\to 0^+}\frac{i}{\pi}\int dE\frac{\gamma_r^+(E)}{\hbar\omega + E - \Delta_N + i\eta}, \quad (25)$$

where $\Delta_N = V(N+1) - V(N)$ is the charging energy cost of moving one electron from one of the leads onto the island when there are N extra electrons there. The factor $\gamma_r^+(\varepsilon)$ is the inelastic (golden rule) tunneling rate through junction r for electrons tunneling to the island [correspondingly $\gamma_r^-(\varepsilon)$ is the inelastic tunneling rate of electrons tunneling from the island through junction r] given by the expression

$$\gamma_r^\pm(\varepsilon) = \frac{\pi}{\hbar}\sum_n \int dE\rho(\varepsilon + E - eV_r)\rho(E) \times f^\pm(\varepsilon + E - eV_r)f^\mp(E)|T^{rn}|^2, \quad (26)$$

where ρ is the density of states in the reservoir r and on the island, both assumed to be either superconductors or normal metal, $f^+(E)$ is the Fermi distribution, $f^-(E) = 1 - f^+(E)$, T^{rn} is the tunneling matrix element, here assumed to be independent of energy and $V_r = (\mu_r - \mu_I)/e$ is the voltage bias across the r junction. Separating Eq. (25) into real and imaginary parts we get

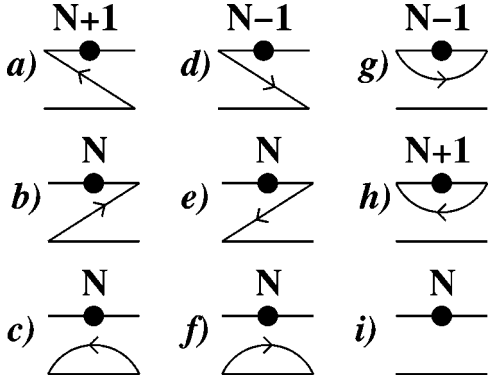

FIG. 7. All the vertex corrections of the external vertex $\hat{N}(\tau)$, denoted by a dot, within the sequential tunneling approximation. Note the correspondence to Fig. 6.

$$D_N = -\sum_r \lim_{\eta\to 0^+} \frac{i}{\pi}\int dE\,\gamma_r^+(E)\left[\frac{\hbar\omega+E-\Delta_N}{(\hbar\omega+E-\Delta_N)^2+\eta^2} - \frac{i\eta}{(\hbar\omega+E-\Delta_N)^2+\eta^2}\right]. \tag{27}$$

The real part of the integral is small in the tunnel limit where the conductance is small, so we neglect these renormalization effects (see Ref. 14) and concentrate on the imaginary part, which gives

$$D_N = -\sum_r \gamma_r^+(\Delta_N - \hbar\omega). \tag{28}$$

Introducing the notation

$$\gamma_N^+(\omega) = \sum_{r=R,L} \gamma_r^+(\Delta_N - \hbar\omega),$$

$$\gamma_N^-(\omega) = \sum_{r=R,L} \gamma_r^-(\Delta_{N-1} + \hbar\omega), \tag{29}$$

all the diagrams in Fig. 6 can be calculated in the same way, resulting in

$$\begin{aligned}
&(a)\Rightarrow \gamma_N^+(\omega), \quad (d)\Rightarrow \gamma_N^-(\omega), \quad (g)\Rightarrow -\gamma_N^-(\omega),\\
&(b)\Rightarrow \gamma_N^+(-\omega), \quad (e)\Rightarrow \gamma_N^-(-\omega), \quad (h)\Rightarrow -\gamma_N^+(\omega),\\
&(c)\Rightarrow -\gamma_N^-(-\omega), \quad (f)\Rightarrow -\gamma_N^+(-\omega), \quad (i)\Rightarrow \frac{i}{\omega}.
\end{aligned} \tag{30}$$

In the same way, the vertex corrections in Fig. 7 can be calculated yielding

$$\begin{aligned}
&(a)\frac{i}{\omega}[\gamma_N^+(0)-\gamma_N^+(\omega)], \quad (d)\frac{i}{\omega}[\gamma_N^-(0)-\gamma_N^-(\omega)], \quad (g)-\frac{i}{\omega}[\gamma_N^-(0)-\gamma_N^-(\omega)],\\
&(b)\frac{i}{\omega}[\gamma_N^+(0)-\gamma_N^+(-\omega)], \quad (e)\frac{i}{\omega}[\gamma_N^-(0)-\gamma_N^-(-\omega)], \quad (h)-\frac{i}{\omega}[\gamma_N^+(0)-\gamma_N^+(\omega)],\\
&(c)-\frac{i}{\omega}[\gamma_N^-(0)-\gamma_N^-(-\omega)], \quad (f)-\frac{i}{\omega}[\gamma_N^+(0)-\gamma_N^+(-\omega)], \quad (i)1,
\end{aligned} \tag{31}$$

where the expression (i) in Eq. (31) corresponds to the zeroth order correction of the vertex. To lowest order, the total spectral density can be written

$$\begin{aligned}
S_V(\omega) &= 2\frac{e^2}{C^2}\mathrm{Re}\left\{\sum_{N,N',N''} P_N^{\mathrm{st}}\hat{V}_{N,N'}(\omega)\hat{\Pi}_{N',N''}(\omega)N''\right\}\\
&= 2\frac{e^2}{C^2}\mathrm{Re}\{\vec{N}^T\hat{\Pi}(\omega)\hat{V}(\omega)\vec{P}^{\mathrm{st}}\},
\end{aligned} \tag{32}$$

where $\vec{N}$ and $\vec{P}^{\mathrm{st}}$ are column vectors ($\vec{N}^T$ is the transpose of $\vec{N}$) containing the number of extra electrons on the island and the steady-state probabilities, respectively. Note thus that the element P_0^{st} refers to the steady-state probability of the SET to be in the state with 0 extra charges, unlike for the qubit, where $P_0^{\mathrm{st,qb}}$ refers to the steady-state probability of being in the lower energy eigenstate. $\hat{V}(\omega)$ is a matrix whose elements $\hat{V}_{N',N}(\omega)$ are the sum of all vertex corrections in Fig. 7 which take the system from the state N to the state N' and $\hat{\Pi}(\omega)$ is a matrix whose elements $\hat{\Pi}_{N'',N'}(\omega)$ are the sum of all diagrams in Fig. 6 that take the system from the state N' to the state N''. Incidentally, Eq. (32) is valid for arbitrary order, as long as the vertex correction and the propagator are dressed to the appropriate order.

In order to facilitate the evaluation of higher order diagrams we define an irreducible diagram as a diagram where it is impossible to draw an auxiliary vertical line at any time, without crossing an electron-hole line. An example can be seen in Fig. 8.

The diagrams in Fig. 6 are all the first order irreducible diagrams, except Fig. 6(i), which is just the free propagator $\hat{\Pi}^{(0)}_{N,N'}(\omega) = (i/\omega)\,\delta_{N,N'}$, where $\delta_{N,N'}$ is a Kronecker delta.

Using irreducible diagrams allows us to write down a matrix Dyson equation in frequency space for the frequency dependent propagator $\hat{\Pi}(\omega)$ between different charge states (Fig. 9)

$$\hat{\Pi}(\omega) = \hat{\Pi}^{(0)}(\omega) + \hat{\Pi}^{(0)}(\omega)\hat{\Sigma}(\omega)\hat{\Pi}(\omega). \tag{33}$$

Solving for $\hat{\Pi}(\omega)$ and inserting the explicit form of $\hat{\Pi}^{(0)}(\omega)$ we get

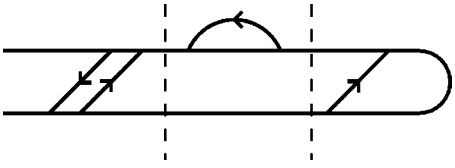

FIG. 8. This diagram contains three irreducible diagrams as in between it is possible to draw a vertical auxiliary line (dashed lines) separating them.

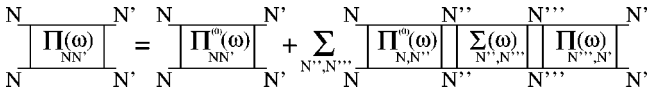

FIG. 9. A graphical representation of the Dyson equation in Eq. (34). The terms $\Sigma_{NN'}$ are irreducible diagrams that take the system from the state N to the state N'.

$$\hat{\Pi}(\omega)=\frac{i}{\omega}\left(\mathbf{1}-\frac{i\hat{\Sigma}(\omega)}{\omega}\right)^{-1}. \tag{34}$$

Note that the explicit time ordering in every diagram, means that in frequency space any specific diagram can be written as a product of irreducible diagrams and free propagators.

The matrix element $\hat{\Sigma}_{N',N}(\omega)$ of the irreducible propagator (self-energy) $\hat{\Sigma}(\omega)$ is the sum of the irreducible diagrams that take the system from the state N to the state N' and $\mathbf{1}=\delta_{N,N'}$ is the unit matrix with the same dimension as $\hat{\Sigma}(\omega)$. Note that the frequency dependence comes directly from the Laplace transform over the time τ, which introduces an auxiliary line with energy $\hbar\omega$. All diagrams located between the times $t=\tau$ and $t=0$ therefore depend on ω.

A. The self-energy $\hat{\Sigma}(\omega)$

The Dyson equation allows us to appropriately sum up the diagrams to a certain order by calculating the self-energy to that order and then inserting it into Eq. (34). As the reservoirs are assumed to be in local equilibrium, we chose to include only diagrams containing at most one electron-hole excitation at any given time. This approximation corresponds to keeping the irreducible diagrams where any vertical line cuts at the most one internal line. This is equivalent to the sequential tunneling approximation leading to the Master equation of orthodox SET theory. The diagrams entering the self-energy to this order are all drawn in Figs. 6(a)–6(h).

B. Vertex corrections

To calculate the noise spectral density we also need to sum all vertex corrections to the same order. As the sequential tunneling approximation only includes terms with at most one tunneling event at a time, all the vertex corrections that enter are those drawn in Fig. 7.

C. Main result

All diagrams which enter Eq. (24) within our approximations are drawn in Fig. 10. Adding them together gives

$$\begin{aligned}S_V(\omega)=\frac{2e^2}{C^2}\sum_N P_N^{\mathrm{st}}\mathrm{Re}\Big\{N\Lambda_N-\frac{i}{\omega}[(N+1)\gamma_N^+(\omega)\\ +N\gamma_N^+(-\omega))\Big](\Lambda_{N+1}-\Lambda_N)\\ -\frac{i}{\omega}[(N-1)\gamma_N^-(\omega)+N\gamma_N^-(-\omega)](\Lambda_{N-1}-\Lambda_N),\end{aligned} \tag{35}$$

where $\Lambda_N=\Sigma_{N'}N'\Pi_{N',N}(\omega)$ and P_N^{st} is the steady-state probability of there being N extra electrons on the island. In Eq. (35) we have used that the steady-state probabilities fulfill the relation $P_{N+1}^{\mathrm{st}}=[\gamma_N^+(0)/\gamma_{N+1}^-(0)]P_N^{\mathrm{st}}$ (see, for instance Ref. 16).

The first term in Eq. (35) corresponds to the result in Eq. (27) of Ref. 13 but with frequency-dependent tunneling rates, while the other terms originate from the vertex corrections. The asymmetry in the noise with respect to positive and negative frequencies arises solely from these vertex corrections. In the limit $\omega\to 0$ Eq. (35) coincides with the zero-frequency limit given in Ref. 13. Note that the frequency-independent terms in the vertex corrections cancel.

Using the relation $\mathrm{Re}\{\hat{\Pi}(\omega)\}=-(1/\omega)\hat{\Sigma}(\omega)\mathrm{Im}\{\hat{\Pi}(\omega)\}$ [this is the real part of Eq. (33), using that the free propagator and the first order self energies are purely imaginary] Eq. (35) can be rewritten in matrix form, which gives the main result in this paper,

$$S_V(\omega)=\frac{2e^2}{C^2}\vec{N}^T\left[\mathbf{1}+\left(\frac{\hat{\Sigma}(\omega)}{\omega}\right)^2\right]^{-1}\frac{\hat{\gamma}(\omega)}{\omega^2}\vec{P}^{\mathrm{st}}, \tag{36}$$

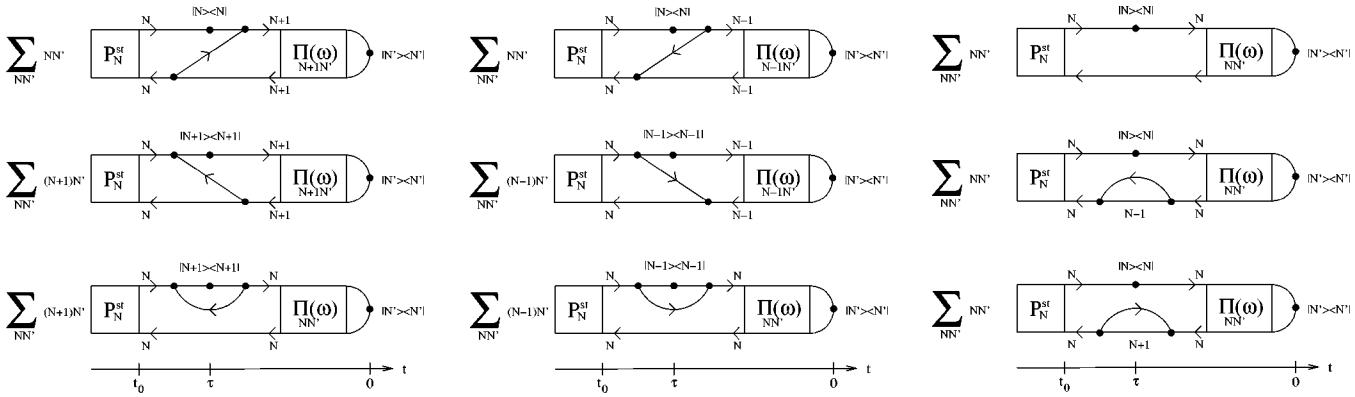

FIG. 10. The sum of all diagrams within the sequential tunneling approximation. The propagators $\Pi_{NN'}$, which is the sum over all the diagrams that take the system from the state N to the state N', are calculated using a Dyson equation (drawn graphically in Fig. 9).

where $\hat{\gamma}(\omega)$ is a tridiagonal matrix whose elements are $\hat{\gamma}_{N,N}(\omega)=\gamma_N^-(\omega)-\gamma_N^+(\omega)$, $\hat{\gamma}_{N+1,N}(\omega)=\gamma_N^+(\omega)$ and $\hat{\gamma}_{N-1,N}(\omega)=-\gamma_N^-(\omega)$.

Note that contrary to $\hat{\Sigma}(\omega)$, $\hat{\gamma}(\omega)$ is not symmetric in frequency and for negative frequencies larger than the maximally available energy from the SET $\hat{\gamma}(\omega)$ is analytically zero while for positive frequencies, $\hat{\gamma}(\omega)$ does not tend to zero but to a finite value.

V. BACK-ACTION DURING MEASUREMENT

When measuring with the SET, the bias voltage is typically large enough to allow for a dc current through the SET but not much larger, which implies that only the charge states 0 and 1 have a nonzero steady-state probability. In this case they are given by $P_0^{\rm st}=\gamma_1^-(0)/[\gamma_1^-(0)+\gamma_0^+(0)]$ and $P_1^{\rm st}=\gamma_0^+(0)/[\gamma_1^-(0)+\gamma_0^+(0)]$. We assume $\Delta_0^L<0$, $\Delta_0^R>0$, and $|\Delta_0^L|>|\Delta_0^R|$ so that electrons typically tunnel from the left to the right, and there is a finite dc current through the SET. We will use these assumptions about the bias throughout the remaining part of the paper, except in the section about the off-state noise of the normal state SET.

A. Low-frequency regime

In the low-frequency regime, defined as the regime where $\gamma_0^-(\omega)$ and $\gamma_1^+(\omega)$ are exponentially small, the charge states 0 and 1 are the only states energetically accessible, also taking into account the externally available energy $\hbar\omega$. In this case the matrix inversion in Eq. (36) is easy to calculate analytically and the noise spectral density is given by

$$S_V(\omega)=\frac{2e^2}{C^2}\,\frac{P_0^{\rm st}\gamma_0^+(\omega)+P_1^{\rm st}\gamma_1^-(\omega)}{\omega^2+[\gamma_0^+(\omega)+\gamma_0^+(-\omega)+\gamma_1^-(\omega)+\gamma_1^-(-\omega)]^2}. \tag{37}$$

This expression has a very simple form: The sum of the steady state probabilities weighted by the inelastic tunneling rates for transitions away from the state, normalized by a denominator containing the finite lifetimes of the states. For zero frequency this corresponds to classical telegraph noise. Note that Eq. (37) is valid both in the normal and superconducting states, the difference only entering in the expressions for the rates $\gamma_{0,1}^{\pm}(\omega)$.

B. High-frequency regime

In the high-frequency limit the spectral noise density of the SET should be independent of the bias and be dominated by the Nyquist noise, which in this regime ($\hbar\omega\gg k_BT$) is[17]

$$S_V^{\rm Nyq}(\omega)=2\hbar\omega\,{\rm Re}\{Z(\omega)\}=\frac{2\hbar\omega R_{||}}{1+(\omega R_{||}C)^2}, \tag{38}$$

where $Z(\omega)$ is the impedance of the SET island to ground and $R_{||}=(1/R_T^L+1/R_T^R)^{-1}$. In this limit $\hat{\Sigma}(\omega)\ll\omega$ and the matrix inversion in Eq. (36) can be Taylor expanded and approximated by the first term $i/\omega[\mathbf{1}+(\hat{\Sigma}(\omega)/\omega)^2]^{-1}\approx(i/\omega)\mathbf{1}$. Still assuming the voltage bias to be small enough to keep only the steady-state probabilities $P_0^{\rm st}$ and $P_1^{\rm st}$ nonzero, Eq. (36) gives

$$S_V(\omega)=\frac{2e^2}{C^2}\,\frac{P_0^{\rm st}[\gamma_0^+(\omega)+\gamma_0^-(\omega)]+P_1^{\rm st}[\gamma_1^-(\omega)+\gamma_1^+(\omega)]}{\omega^2}. \tag{39}$$

In the high-frequency limit, $\hbar\omega\gg\{E_C,eV\}$, all rates are similar and they are proportional both to the normal state tunnel conductance and the frequency

$$\gamma_0^{\pm}(\omega)\approx\gamma_1^{\pm}(\omega)=\frac{\hbar\omega}{2e^2}\left[\frac{1}{R_T^L}+\frac{1}{R_T^R}\right]+O(1), \tag{40}$$

where $O(1)$ indicates a bias-dependent constant. This is valid both in the normal and superconducting states. It is clear that inserting Eq. (40) into Eq. (39) gives Eq. (38). It might be interesting to note that it is enough to include four charge states to recover the full Nyquist noise. If only two charge states were included, an extra charge on the island would prevent further electrons to tunnel until the extra electron has left the island, and the correlation effectively would reduce the noise to that of a single junction. For similar reasons, for intermediate frequencies the noise should be reduced, compared to the Nyquist noise.

C. Normal state SET

For an SET operated in the normal state, the density of states can be assumed to be energy independent when calculating the tunneling rates in Eq. (26). Using $\rho_{I,n}(E)=\rho_{r,n}(E)=\rho_N$, the tunneling rates $\gamma^{\pm}(\omega)$ can be written

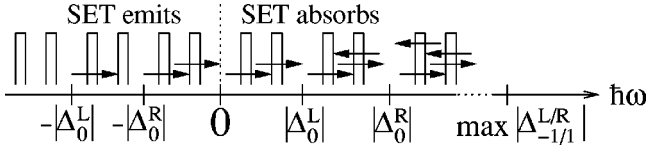

FIG. 11. A schematic picture of the different processes in the SET for different frequencies. Note that negative frequencies correspond to processes where the SET emits energy, while positive frequencies correspond to processes where the SET absorbs energy.

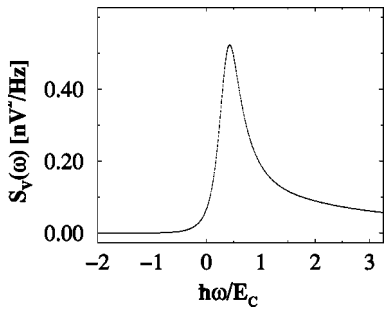

FIG. 12. Spectral noise density for an SET run in normal mode. The calculation was done for zero temperature and with symmetric tunnel junctions $R_R = R_L = 21.5$ kΩ. The dc current through the SET was 1.5 nA, $n_x = 0.25$, $E_C = 2.5$ K.

$$\gamma_N^+(\omega) = \frac{\pi}{\hbar} \sum_r \alpha_0^r \Gamma^+(\Delta_N^r - \hbar\omega), \tag{41}$$

$$\gamma_N^-(\omega) = \frac{\pi}{\hbar} \sum_r \alpha_0^r \Gamma^-(\Delta_{N-1}^r + \hbar\omega), \tag{42}$$

where $\alpha_0^r = \Sigma_n |T^{rn}|^2 \rho_N^2 = R_k/4\pi^2 R_T^r$ is the dimensionless conductivity (R_k is the quantum resistance and R_T^r is the tunneling resistance of junction r), $\Gamma^-(E) = E/[1-\exp(-\beta E)]$, $\Gamma^+(E) = E\exp(-\beta E)/[1-\exp(-\beta E)]$, and $\beta = 1/k_B T$. Note that Δ_N^r includes both charging and biasing energies.

At zero temperature, the $\Gamma^{\pm}$ become step functions multiplied by a linear term $\Gamma^-(E) = |E|\,\theta(E)$, $\Gamma^+(E) = |E|\,\theta(-E)$. In this limit the rates are easy to analyze.

For frequencies of small magnitudes $|\hbar\omega| < |\Delta_1^r|, |\Delta_{-1}^r|$ only the charge states $|0\rangle$ and $|1\rangle$ are energetically allowed and we can use Eq. (37) to calculate the noise spectral density. Even though the expression in Eq. (37) looks very similar to the classical expression with frequency dependent rates, this frequency dependence of the rates changes the behavior quite drastically. The spectral noise density is no longer symmetric with respect to ω, and there is a finite maximum energy available for emission from the SET, which can be seen in Fig. 12 as $S_V = 0$ for large negative frequencies $\hbar\omega < -|\Delta_0^L|$. This means that if the energy splitting of the qubit is larger than the energy gained by putting an extra electron on the island (Δ_0^L), there is not enough energy available from the SET to excite the qubit, and the SET behaves as a passive load, only able to absorb energy.

The preference of the SET to absorb energy rather than emit is also clear as $S_V(\omega) > S_V(-\omega)$ for any $\omega > 0$. This means that any two-level system with finite energy splitting driven to steady-state solely by the SET will not have an equal steady-state probability of both states.

1. Low-frequency regime

For low frequencies $|\hbar\omega| < |\Delta_0^R|$ when no backward tunneling processes are allowed (see Fig. 11), the noise spectral density can be written

$$S_V(\omega) = \frac{e^2}{C^2} \frac{2I/e + 2\pi\omega[P_0^{\rm st}\alpha_0^L + P_1^{\rm st}\alpha_0^R]}{\omega^2 + 4[\gamma_0^+(0) + \gamma_1^-(0)]^2}, \tag{43}$$

where the first term in the numerator $I = 2e\gamma_0^+(0)\gamma_1^-(0)/[\gamma_0^+(0) + \gamma_1^-(0)]$ is the dc current through the SET. We see that the difference compared with classical telegraph-noise is the term linear in ω in the nominator. This is a quantum mechanical correction originating from the vertex corrections. In this regime the frequency dependent part of the tunneling rates in the denominator cancel.

In the symmetrized noise $S_V^{\rm sym}(\omega) = S_V(\omega) + S_V(-\omega)$, the linear term in the numerator cancels out. Thus in this region, for quantities that are proportional to the symmetrized noise, such as the mixing time [see Eq. (14)], the classical telegraph noise give the same result. But for other quantities, such as the steady-state probabilities of a qubit driven by the SET [see Eq. (10) and Eq. (11)], the difference is evident even for small frequencies.

2. Coulomb staircase

Using the SET to measure the average charge of the Cooper-pair box qubit it is reasonable to assume that the back action from the SET is the dominant noise source. At the degeneracy point of the qubit, the energy splitting between its two eigenstates is E_J. If $E_J < \Delta_0^R$ we can use Eq. (43) to calculate the Coulomb staircase [Eq. (12)] close to the degeneracy as

$$\langle Q\rangle = e\left[1 + \frac{8E_c\pi\alpha_0}{\hbar I/e}\delta n_g\right] = e\left[1 + \frac{4E_c}{eR_T I}\delta n_g\right], \tag{44}$$

where δn_g is the deviation from the degeneracy point ($n_g = 1/2$) and we have assumed symmetric junctions ($\alpha_0^L = \alpha_0^R = \alpha_0$ or $R_T^L = R_T^R = R_T$) and a symmetric voltage bias in the SET. Thus, close to the degeneracy, we will always get a linear charge increase for suitable choice of SET bias. In this regime the derivative is thus determined by the current through the SET rather than the Josephson energy in the qubit.

Away from the degeneracy point, when the energy splitting of the qubit is increased, the low-frequency requirement for Eq. (43) may not be fulfilled. In order to calculate the influence from the noise on the Coulomb staircase for arbitrary qubit gate voltage we have to include the full expression from Eq. (35). The result for a typical setup is plotted in Fig. 13, demonstrating that the back-action noise from the SET introduces additional smearing of the Coulomb staircase. This can be compared to the results by Nazarov,[18] where the influence of the back action of an SET in the normal state is calculated on a small metallic island in the normal state.

3. Mixing time

Using the tunneling rates in Eqs. (41),(42) and inserting them into Eq. (35) we can calculate the mixing time $\tau_{\rm mix}$ due

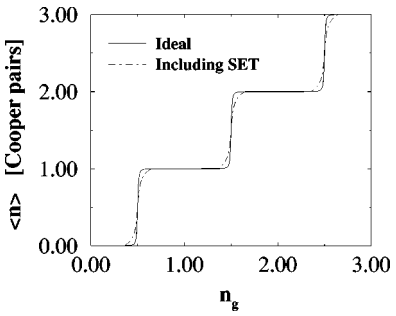

FIG. 13. The Coulomb staircase of an SCB driven to steady state by the SET run in normal state. The parameters we have used for the SCB are $E_{\rm qb}=2.5$ K, $E_J=0.1$ K, $\Delta=2.5$ K and for the SET we have used $E_C=2.5$ K, $R_R=R_L=21.5$ kΩ, and $n_x=0.25$.

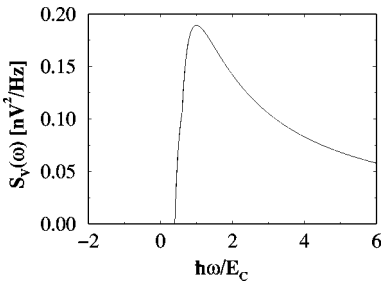

FIG. 15. Noise spectral density of an SET in the off state. Note that only contributions from positive frequencies remain, as no energy can be emitted from the SET within the sequential tunneling approximation. The noiseless region is given by $\Delta_0^l-\hbar\omega>0$.

to the voltage fluctuation on the SET-island as a function of the energy splitting. Using a state-of-the-art rf-SET (Ref. 19) coupled to a qubit with realistic parameters (see caption), as shown in Fig. 14, this would give a mixing time of approximately 10 μs. This should be compared with the measurement time $t_{\rm ms}$ needed to resolve the two charge states in the same setup which is about 0.4 μs. The resulting signal-to-noise ratio (SNR) is SNR$=\sqrt{\tau_{\rm mix}/t_{\rm ms}}\approx 5$, which indicates that single-shot read out is possible.

4. Off-state noise—Qubit reset

One property of the SET used as a charge qubit read-out device is that it may be switched off by lowering the driving bias so that sequential tunneling is no longer possible, i.e., both $0<\Delta_0^L$ and $0<\Delta_0^R$. In this regime the voltage noise is determined by cotunneling processes.[20] Since cotunneling is a second order process in the tunneling conductance the voltage noise in the off state[4,21] is several orders of magnitude smaller than the on-state noise.

Taking energy exchange with the qubit into account there may be a first order tunneling event in the SET, even though the driving bias is too small for sequential tunneling. The energy taken from relaxing the qubit may stimulate a photon-assisted first-order tunnel event in the SET. At zero temperature the condition for such an event is simply $\Delta E>\min\{\Delta_0^L,\Delta_0^R\}$. The voltage noise spectral density of the SET in the off state is shown in Fig. 15. The curve has been calculated using Eq. (35), with $P_0^{\rm st}=1$. This implies that in order to benefit from the low voltage fluctuations in the off-state the SET should be switched off by switching both the driving bias to zero and using the SET gate voltage to put it far into the Coulomb cotunneling regime, i.e., $n_x\approx 0$.

The nonlinearity of the voltage noise spectral density may also be used for fast relaxation of the qubit, i.e., as a qubit reset button. If the gate voltage of the SET is such that $\Delta E\geqslant|\Delta_0^L|\approx\Delta_0^R$, and the driving bias is zero, the qubit relaxation rate is first order in the tunnel conductance, while the excitation rate is given by cotunneling. The normal state SET may thus be used for qubit reset, or in other words as a switchable dissipative environment to the qubit.

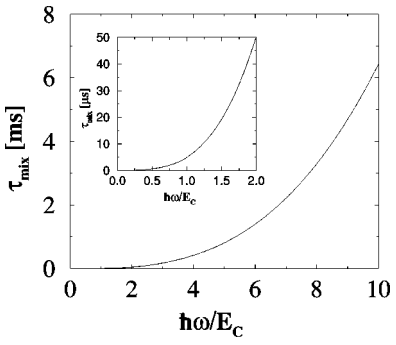

FIG. 14. The mixing time of an SCB caused by the SET. The inset shows an expanded view around $\hbar\omega\approx E_{\rm qb}$. Thus, for an energy splitting of the qubit of approximately $E_{\rm qb}$, the mixing time is around 10 μs. The parameters used were $E_C=2.5$ K, $E_{\rm qb}=0.8$ K, $E_J=0.15$ K, $R_R=R_L=21.5$ kΩ, $\kappa=0.01$, $I_{dc}=9.6$ nA.

D. Superconducting SET

Compared with a normal state SET (NSET) the superconducting SET (SSET) shows two main differences. The density of states in the reservoirs is changed by the superconducting energy gap Δ, and in addition to quasiparticle tunneling also Cooper pair tunneling may occur. We will consider an SSET biased so that sequential quasiparticle tunneling is allowed, and in this regime Cooper pair tunneling may be neglected. Thus the same model as before can be used, only taking into account the changed quasiparticle density of states. As we are interested in an SET made out of aluminum, we use the BCS density of states

$$\rho(E)=\rho_N\frac{|E|}{E^2-\Delta^2}\,\theta(|E|-\Delta), \tag{45}$$

where ρ_N is the density of states of the normal state. Inserting these into the expression for the tunneling rates in Eq. (26) we get for zero temperature (see, e.g., Ref. 22)

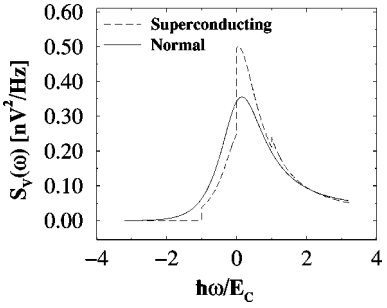

FIG. 16. Comparing the spectral noise density for a superconducting and a normal conducting SET. The parameters used were $R_L=R_R=21.5$ kΩ, $E_C=2.5$ K, $n_x=0.25$, and $I_{dc}=9.6$ nA.

$$\gamma_r^{\pm}(w)=\frac{\pi}{\hbar}\frac{\alpha_0^r\theta(\mp\hbar\omega\pm eV_r-2\Delta)}{2\Delta\mp\hbar\omega\pm eV_r}\times\left[(\hbar\omega-eV_r)^2\mathbf{K}\left(\frac{\hbar\omega-eV_r\pm2\Delta}{\hbar\omega-eV_r\mp2\Delta}\right)-(2\Delta\mp\hbar\omega\pm eV_r)^2\left\{\mathbf{K}\left(\frac{\hbar\omega-eV_r\pm2\Delta}{\hbar\omega-eV_r\mp2\Delta}\right)-\mathbf{E}\left(\frac{\hbar\omega-eV_r\pm2\Delta}{\hbar\omega-eV_r\mp2\Delta}\right)\right\}\right],$$

where $\mathbf{K}(x)$ and $\mathbf{E}(x)$ are elliptic integrals of the first and second kind. These rates behave just as the *IV* curve for an *SIS* junction. The singularities in the superconducting density of states introduce discontinuities into the tunneling rates. These discontinuities will also introduce discontinuities in the noise spectral density.

Comparison between an SSET and an NSET. Comparing the noise spectral density of an NSET and an SSET (see Fig. 16) is not completely straightforward as the SSET requires considerably higher voltage bias in order to get sequential quasiparticle tunneling through the SET, i.e. $|eV_L-eV_R|>4\Delta+E_C(1-2n_x)$. Therefore when comparing these two in the on state (i.e. while measuring), we use the same tunnel conductance and gate voltage, and then choose a voltage bias that gives the same dc current through the two SET's. This is motivated by the fact that the zero frequency noise is determined by the dc current through the SET, this biasing therefore yields the same zero frequency telegraph noise for both the SSET and the NSET.

Apart from the discontinuities in the spectral density of the SSET, the finite frequency noise differs in another important aspect. Although the two SET's carry the same dc current, the processes producing that current are qualitatively different. In the superconducting SET biased just above the threshold the energy gain in each single tunnel event is quite small, determined by approximately $\max\{|eV_L|,|eV_R|\}-2\Delta$. The relatively large current is an effect of the divergent density of state peaks in the reservoirs. In the normal state SET carrying the same current the maximum energy that may be extracted from a single tunneling event is instead quite large, proportional to $\max\{|eV_L|,|eV_R|\}$.

Comparing the voltage noise spectral density for negative frequencies, capable of exciting the measured system, we find that the SSET noise is zero for $\hbar\omega<-(\max\{|eV_L|,|eV_R|\}-2\Delta)$, while the NSET spectrum extends down to $\hbar\omega\approx-\max\{|eV_L|,|eV_R|\}\approx-2\Delta$.

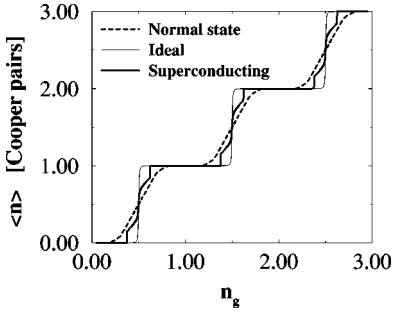

FIG. 17. Comparison of an ideal Coulomb staircase and a staircase where the qubit is driven to steady state by either an SET in the normal or in the superconducting state. We have use the same parameters as in Fig. 13.

Measuring the Coulomb staircase with an NSET and an SSET biased to the same dc current will thus give different results. The Coulomb staircase is sharper for the SSET because the lower amount of energy extractable from the SET reduces the excitation rate for the two-level system, and the discontinuities in the noise spectral density of the SSET are also clearly visible, as seen in Fig. 17. Even though this is a completely different bias regime, similar structure appears in Ref. 23.

Note that the staircases in Fig. 17 has been calculated for zero temperature and for a fixed voltage bias across the SET, and that the dc current is different in Figs. 17 and 13. When calculating the total mixing time, the sum of relaxation and absorption rates enters, and the difference between an SSET and an NSET diminishes. The lower tendency for the superconducting SET to emit is compensated for by an increased tendency to absorb energy.

Since the mixing time due to an SSET dependends on the sum of the contributions from absorptive and emissive processes, it is thus not very different from an NSET carrying the same dc current. An example can be seen in Fig. 18.

VI. CONCLUSIONS

We have calculated the full frequency spectral density of voltage fluctuations in a single electron transistor (SET),

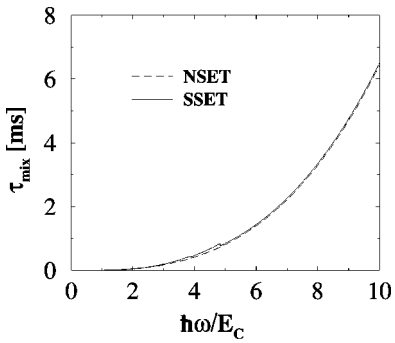

FIG. 18. The mixing time due to the noise from the SET run either in the normal state or in the superconducting state, using the same dc current through the SET (approximately 10 nA).

used as an electrometer biased above the Coulomb threshold so that the current through the SET is carried by sequential tunneling events. We take the energy exchange between the SET and the measured system into account using a real-time diagrammatic Keldysh technique. We find simple analytical expressions for the noise in the low- and high-frequency regimes and in between we calculate the noise numerically. The complexity of the numerical calculation is limited to the inversion of a NXN matrix where N is the number of charge states involved, typically $N \leqslant 5$.

Previous expressions for the voltage fluctuations, where the energy exchange is not taken into account, are by definition symmetric with respect to positive and negative frequencies. We show that there is an asymmetry, technically arising from the first order vertex corrections of the external vertices, so that the noise capable of exciting the measured system is always less than the noise that will relax the measured system, at any given frequency. The importance of this difference is shown by calculating the Coulomb staircase of a Cooper pair box, as measured by the SET. Interestingly the difference has a tendency to cancel in the expression for the symmetric noise, i.e., the sum of the positive and negative frequency noise. This implies that the classical calculation is a reasonably good approximation for that quantity.

The divergence in the superconducting density of states results in discontinuities in the voltage noise spectral density of the superconducting SET (SSET). Compared to a normal state SET carrying the same DC current the SSET also has considerably less ability to excite the measured system.

ACKNOWLEDGMENTS

We gratefully acknowledge rewarding discussions with Per Delsing, David Gunnarsson, Kevin Bladh, Vitaly Shumeiko, Alexander Zazunov, Alexander Shnirman, and Yuriy Makhlin. This work was partially funded by the Swedish grant agency NFR/VR and by the SQUBIT project of the IST-FET program of the EC.

[1] A. Aassime, G. Johansson, G. Wendin, R. J. Schoelkopf, and P. Delsing, Phys. Rev. Lett. **86**, 3376 (2001).
[2] B. E. Kane, N. S. McAlpine, A. S. Dzurak, R. G. Clark, G. J. Milburn, He Bi Sun, and Howard Wiseman, Phys. Rev. B **61**, 2961 (2000).
[3] M. J. Lea, P. G. Frayne, and Y. Mukharsky, Fortschr. Phys. **48**, 1109 (2000).
[4] D. V. Averin, *Macroscopic Quantum Coherence and Quantum Computing*, edited by D. V. Averin, B. Ruggiero, and P. Silvestrini (Kluwer, New York, 2001), pp. 399–407.
[5] Y. Makhlin, G. Schön, and A. Shnirman, Phys. Rev. Lett. **85**, 4578 (2000).
[6] R. J. Schoelkopf, P. Wahlgren, A. A. Kozhevnikov, P. Delsing, and D. E. Prober, Science **280**, 1238 (1998).
[7] V. Bouchiat, D. Vion, P. Joyez, D. Esteve, and M. H. Devoret, Phys. Scr. **T76**, 165 (1998).
[8] Y. Nakamura, Y. A. Pashkin, and J. S. Tsai, Nature (London) **398**, 786 (1999).
[9] G. Johansson, A. Käck, and G. Wendin, Phys. Rev. Lett. **88**, 046802 (2002).
[10] R. Aguado and L. P. Kouwenhoven, Phys. Rev. Lett. **84**, 1986 (2000).
[11] M. H. Devoret and R. J. Schoelkopf, Nature (London) **406**, 1039 (2000).
[12] Y. Makhlin, G. Schön, and A. Shnirman, Rev. Mod. Phys. **73**, 357 (2001).
[13] A. N. Korotkov, Phys. Rev. B **49**, 10 381 (1994).
[14] H. Schoeller and G. Schön, Phys. Rev. B **50**, 18 436 (1994).
[15] H. Schoeller, *Mesoscopic Electron Transport* (Kluwer Academic Publishers, Dordrecht, 1997), p. 291.
[16] G. R. Grimmett and D. R. Stirzaker, *Probability and Random Processes* (Oxford Science Publications, Oxford, 1992).
[17] H. B. Callen and T. A. Welton, Phys. Rev. **83**, 34 (1951).
[18] Y. V. Nazarov, J. Low Temp. Phys. **90**, 77 (1993).
[19] A. Aassime, D. Gunnarsson, K. Bladh, P. Delsing, and R. Shoelkopf, Appl. Phys. Lett. **79**, 4031 (2001).
[20] D. V. Averin and A. A. Odintsov, Phys. Lett. A **140**, 251 (1989).
[21] A. M. van den Brink, Europhys. Lett. **58**, 562 (2002).
[22] M. Tinkham, *Introduction to Superconductivity* 2nd ed. (McGraw-Hill, New York, 1996).
[23] A. A. Clerk, S. M. Girvin, and A. D. Stone, Phys. Rev. Lett. **89**, 176804 (2002).